# Feasibility of SD-OCT via Acousto-Optics

Anonymous 15-862 Computational Photography submission

Paper ID 0001

## Abstract

*This project aims to examine the feasibility of spectral domain optical coherence tomography (SD-OCT) via Acousto-Optics. Having eclipsed its time domain counterpart due to its enhanced time resolution and intrinsic noise level, SD-OCT has become increasingly popular in clinical applications. The drawback of OCT lies in its signal-to-noise ratio in scattering media, a property of biological samples. This limits the capability of deep tissue imaging via OCT and leads to more invasive methods. With the help of an active focusing lens in the form of ultrasound transducers, it is feasible to enhance the SNR of SD-OCT to potential functional imaging of biological samples.*

## 1. Introduction

The use of interferometry provides the unique situation where light-light interactions provide information. One of the first instances of such a technique was demonstrated by Michelson in the $19^{th}$ century. The michelson interferometer is a simple setup where light is split by a beam splitter and allowed to travel different path lengths. When the light travels a certain path length, it has a certain phase. If the two beams travel different path lengths, the therefore have different phases. The two beams are reflected by mirrors and the superposition of these two beams reuslt in interference fringe patterns which can be used to extract information about not only the path length difference between the two sources but also the material properties each arm interacts with. This demonstration laid the foundation for several sophisticated interferometry techniques which application in vision, biomedical imaging and sensing.

Optical Coherence Tomography is an imaging technique that leverages principles of interferometry primarily used for imaging tissue. Optical coherence tomography is essentially a Michelson Interferometer that has a sample at the end of one arm instead of a mirror. There have been several developments within the OCT space since its inception. Researchers have been drawn toward spectral domain optical coherence tomography and swept source optical coherence tomography which has a significantly better time resolution when compared to time domain OCT. In the case of spectral domain OCT, a broadband light source is used. Each wavelength in this broadband reflects from different depths of the sample. These wavelength dependent fringes are separated using a spectrometer. Therefore, depth information of a point is obtained much faster than in the case of time domain OCT where the reference arm needs to be scanned to obtain depth information. There have been attempts to perform functional brain imaging non-invasively using OCT. Unfortunately, SD-OCT struggles to deal with highly scattering media that have large depths. The sample arm beam path is focused onto the surface of the plane and the SNR drops considerably with depth. The passive nature of lens based focusing has no way of dealing with the exponential signal drop with increasing depth. This restricts the use of OCT to external layers and deprives this powerful tool of its true potential. Acousto-Optics presents a way to move past this. By being an active optical focusing modality, SD-OCT provides an avenue to mitigate this issue.

## 2. Experimental Setup, OCT Acquisition and Processing

To perform Spectral Domain Optical Coherence tomography, several components need to be assembled as shown in figure 1. The broadband source used is a superluminescent diode centred around $830nm$, having a 3dB bandwidth of $40nm$. This laser source is routed to a 50-50 beam splitter. One arm of the beam splitter forms the reference arm by connecting a collimator, which sends the beam to the reference arm mirror and back. There is a variable attenuator in the reference arm path to match the signal received from the sample arm to maximize the fringe depth of the interference signal. A polarization controller is used for the same purpose. The other output from the beam splitter is sent to a $30mm$ lens via a collimator. The beam converges, diverges and then enters the first facet of the ultrasound transducer. The transducer is cylindrical and its resonant frequency is a function of its thickness. The transducer and light source are connected to a signal generator to pulse the components. A power amplifier is

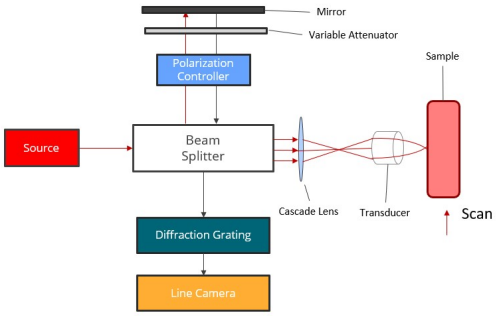


Figure 1. SD-OCT via acousto optics cascade system schematic

used to amplify the signal sent from the signal generator to drive the transducer.

A camera is focused onto the edge of the transducer and then laterally translated to the center of the transducer to examine the plane of the top facet of the transducer as shown in figure 2. This camera can be translated axially to view different planes to view different focusing effects at a variety of planes.

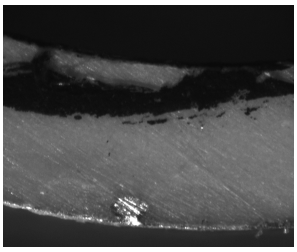

Figure 2. Top Plane of the transducer

The resonant frequency of the transducer is sensitive to the medium in which the transducer operates. The stimulation frequency is swept using the signal generator until a voltage peak is detected from the output of the amplifier, indicating the system is in resonance. The transducer used for this project had a resonance frequency around $1MHz$. The phase difference between the laser and the ultrasound signals is altered so that the laser is in phase with the peak of the pressure waves created by the transducer at resonance. The lower the duty cycle of the laser signal, the better the lateral resolution of the system. Although this is the case, the laser power is reduced in the process, thereby reducing the SNR of the system for the same maximum laser power. Although this is the case, OCT used on biological samples has upper limits on the laser power that is well within the confines of modern laser drivers. The phase difference between the laser and the ultrasound is adjusted to obtain a circular focused spot. The frequency and phase of the transducer are tuned alternatively over multiple iterations to provide the desired focus pattern. The voltage supplied to the piezoelectric material that makes up the transducer defines the plane at which ballistic photons are focused. Figures 3 and 4 illustrate the focusing capability of cylindrical ultrasound transducers.

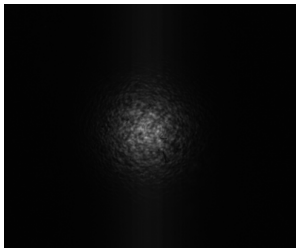

Figure 3. Ultrasound Off

Figure 4. Ultrasound On

Once the desired focus is obtained at the plane of interest, the camera viewing the top facet of the transducer is replaced by a mirror that is identical to the mirror on the reference arm. These mirrors ideally reflect all the light intensity they recieve back to the collimator that sends the light to the mirrors. The reflected waves are sent back to the beam splitter and their interference signal is sent to a diffraction grating that separates this superposition of waves into its wavelength dependent components. A lens is then used to confine the optical beam to a line that can be detected by the line camera. The acquisition of this signal is done via a visual studio solution provided by H. B. Park from UC Riverside. The acquisition program allows visualization of the raw IMAQ of the interference signal as well as its intensity which ultimately forms the OCT image. The angles of the mirrors are adjusted individually to ensure maximum back coupling of the signal on either arm. The signal from each arm should follow that of the SLD spectrum used as the source in the system. An illustration of this is shown in figure 5 which is obtained from the OCT acquisition program. The sample arm amplitude is maximized when the cascade lens causes the entire bottom facet of the transducer to be illuminated. This situation can be achieved by scanning the cascade lens in the axial direction while the transducer is on and the sample arm mirror is in place.

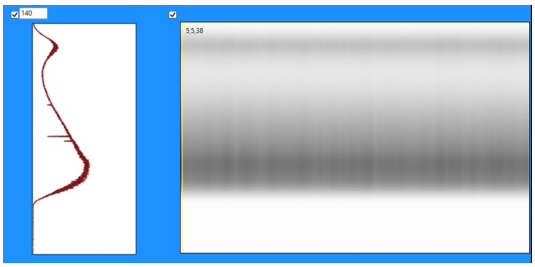

Figure 5. Referance Arm Spectrum

/newline The system requires calibration and dispersion

optimization. The calibration is done by blocking the sample arm and placing a thin cover slip over the reference arm. This provides an interference signal implied by the path length difference caused by the thickness of the cover slip. The peak is observed and selected. A similar procedure is done to characterize the dispersion of the system. The sample arm is unblocked and the cover slip is removed from the reference arm path. The peak is then located and selected. This procedure of calibration and dispersion characterization needs to be redone if any significant changes to the system are made. It is also beneficial to redo this characterization every so often as the concentration of the medium where the sample is immersed could change and thereby change the dispersion characteristics.

Once the individual arm back coupling is optimized, the path lengths of the two arms need to be matched to observe the interference fringe patterns. This can be done by scanning the collimator used on the reference arm in the axial direction. Once the fringes are observed in the raw IMAQ view, the intensity view provides information on the relative location of the mirrors. If the system is well characterized, the mirror intereference appears as a sharp line. The reference arm path length when increased should move this line downward to indicate the correct placement of any potential scan of a sample. Incorrect placement would result in two halves of the sample to overlap with each other, thereby corrputing the image and losing any possible information. The reference arm collimator is scanned axially and the signal to noise ratio roll-off versus depth can be obtained by recording known displacements.

/newline Once the reference arm collimator has been translated to achieve a large window to obtain sample information, its position is then fixed. The sample arm mirror is then replaced by the sample of interest. The sample is typically encased in an agar mould alongside a piece of aluminum foil. The aluminum foil is suspended adjacent to the sample and its purpose is to locate the edge of the sample to be imaged. Once the sample is placed into the system, its angles relative to the transducer are varied until an image of the aluminum foil (mirror-like reflection). The sample is then translated until this strong reflection disappears and is then raster scanned with a scan rate of choice. The scan rate must be slow enough so as to minimize motion blur. In addition to the interference signals, the reference arm signal must be stored as well to extract the sample arm information.

Each depth scan is saved as a .dat file that must be stitched together after the scan is complete during post-processing. The post-processing is done using Matlab. A large amount of the post-processing code has been provided by H. B. Park. The depth scans are read and are stitched together iteratively to create a 2D scan of the sample. This process can be done along multiple scan lines of the sample and then stacked to provide 3D information about the sample.

## 3. Results and Discussion

The SNR roll off of the system can be visualized via plots with the reference arm mirror at different axial positions as shown in figure **??**. The representative plots depict the interference obtained for reference arm collimator at different heights away from where the reference arm path length is matched to that of the sample arm. It can be observed in 6, that the SNR at $1mm$ away from the approximate zero path length difference region, is around 105dB. This signal expectedly trends downwards as we move further away from the zero path length difference region. Figure 8 indicates that the system has a 10dB drop in signal across a range of $4mm$. This roll-off corresponds to conventional lens based SDOCT-systems(Chalmiani et al, 2022).

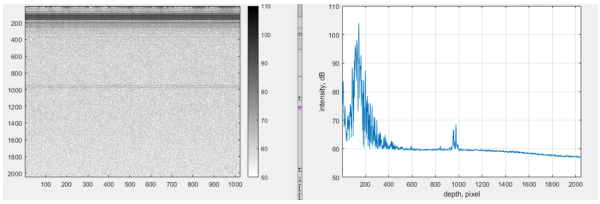

Figure 6. Roll-Off $1mm$

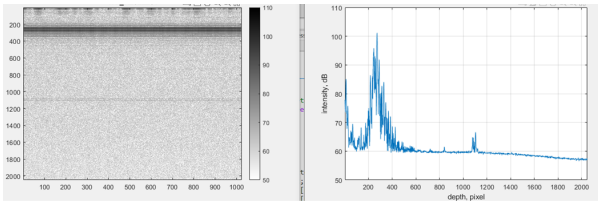

Figure 7. Roll-Off $2mm$

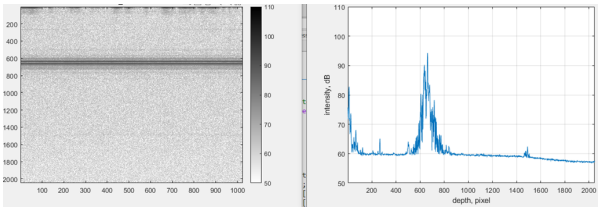

Figure 8. Roll-Off $5mm$

To establish the capability of the system in the context of biological imaging, a mouse paw was chosen as the sample. The mouse paw was de-haired to reduce any interflections and thereby false depth estimation. The bone of the paw and the skin of the paw have contrasting optical properties. The shape of the bone can be estimated as shown in figure 9.

This depth profile shows the signs that the use of acousto-optics in SD-OCT to focus light onto samples is feasible.

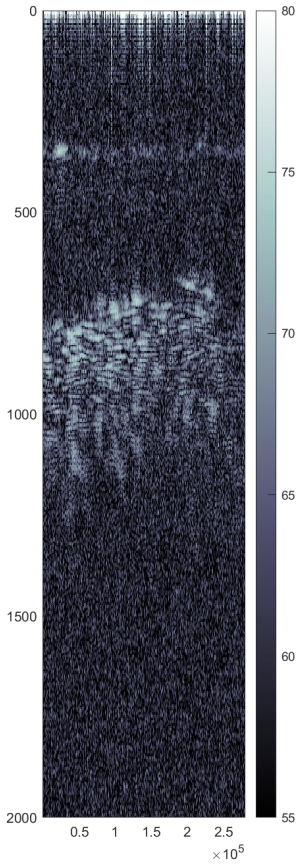


Figure 9. Top Plane of the transducer

Although this is the case, further optimizations could significantly improve the depth estimation of samples. It has been shown that ultrasound pressure waves can guide lightly scattered photons to the plane of interest (Pediredla et al, 2021). By placing a sample within the transducer, these scattered photons can be redirected. A portion of these scattered photons that enhance light throughput will not affect the lateral resolution of the system, there exists a trade-off between the amount of redirected scattered photons that are not within the desired lateral spot size. In addition to this, higher frequency pressure waves result in a larger number of re-directed scattered photons until aberrations become prevalent. A limitation on the negative peak pressure $P$ generated by transducers is posed by the modulation index defined by the equation below.

$$MI = \frac{P}{\sqrt{f}}$$

A modulation index of 1.9 is defined as the safety threshold where the frequency of stimulation $f$ is inversely related. The modulation index is a safety unit to prevent cavitation of the medium. This is another reason why moving the higher frequencies could prove to be valuable. Cylindrical transducers that operate in the thickness mode need to be thinner to resonate at higher frequencies. The diameter of these transducers decreases as their thickness decreases to maintain their structural integrity. As the diameter reduces, the size of the samples that can be placed inside transducers must also be reduced. The use of cylindrical transducers that operate in the thickness mode thereby proves to be a limitation. This limitation can be mitigated by using travelling wave transducers. Unfortunately, travelling wave transducers that can resonate at the sweet spot between scattered photon redirection and aberrations need to operate at higher harmonics of the transducer. This means the pressure generated is significantly less than that of the cylindrical transducers. That being said, it should be possible to focus a significant amount of scattered photons to the region of interest. It is also worth pointing out that the phase difference between the redirected photons and the ballistic photons should be within the time coherence of the system so as to provide an accurate depth estimation. If the redirected photons correspond to different time bins, this will mean that their phase will be different to the ballistic photons reflected from the same depth. The phase of these photons will then cause interference fringes that correspond to different depths of the sample.

Another shortcoming of the cylindrical transducer is that the resonance frequency drifts over time. This is caused due to thermal fluctuations in media. A drift in frequency corresponds to a change in the phase difference between the light source and the positive peak of the ultrasound transducer. The spot size and shape that is focused onto the sample is then compromised. Although the transducer resonant frequency can be tracked without observing the point of focus, the spot size and shape cannot be tracked when the mirror and sample are placed at the end of the sample arm. To mitigate this, a dual transmission and reflection optical path needs to be created. A neutral density filter that is at the plane at the top of the transducer should be observed by a camera focused at this plane to track the best lateral resolution. The neutral density filter can also act as a partial mirror to track the interference signals and maximize fringe depth. During sample imaging, no tuning of amplitude, frequency or phase should be carried out.

As the point spread function of a lens based SD-OCT focus is gaussian and that of the acousto-optics cascade system is bessel, a combination of depth scans can be obtained. Joint bilateral filtering process can be used to transfer sharpness from shallower depths of the lens based SD-OCT using per column computations. This could provide a good inbetween where depth of focus is achieved without compromising lateral resolution. Per pixel operations can be

done to de-blur images by deriving the PSF of either case. Deblurring would not only make the images look prettier but would also significantly contribute towards faster diagnosis of diseases and exploration of functional imaging in the brain.

## 4. Conclusion

This project explores the feasiblity of Acousto-Optics-assisted spectral domain optical coherence tomography. It illustrated multiple approaches that can be taken to further improve the system as well as showed the its capability in imaging real biological tissue.

### 4.1. References

[1] Adithya Pediredla, Matteo Giuseppe Scopelliti, Srinivasa Narasimhan et al. Optimized Virtual Optical Waveguides Enhance Light Throughput in Scattering Media, 17 August 2021, PREPRINT (Version 1) available at Research Square [https://doi.org/10.21203/rs.3.rs-778793/v1]

[2] Yasin Karimi, Hang Yang, Junze Liu, B. hyle Park, and Maysamreza Chamanzar, "Enhanced spectral-domain optical coherence tomography (SD-OCT) using in situ ultrasonic virtual tunable optical waveguides," Opt. Express 30, 34256-34275 (2022)

[3] Yasin Karimi, Matteo Giuseppe Scopelliti, Ninh Do, Mohammad-Reza Alam, and Maysamreza Chamanzar, "In situ 3D reconfigurable ultrasonically sculpted optical beam paths," Opt. Express 27, 7249-7265 (2019)